ECOGRAPHY

Research

Linking variability of tree water use and growth with species resilience to environmental changes

Christoforos Pappas, Richard L. Peters and Patrick Fonti

C. Pappas (https://orcid.org/0000-0001-5721-557X) ✉ (christoforos.pappas@umontreal.ca), Dépt de géographie, Univ. de Montréal, Montreal, QC, Canada, and Faculty of Environmental Sciences, Czech Univ. of Life Sciences Prague, Czech Republic. – R. L. Peters and P. Fonti (https://orcid.org/0000-0002-7070-3292), Forest Dynamics, Swiss Federal Research Inst. for Forest, Snow and Landscape Research WSL, Birmensdorf, Switzerland. RLP also at: Dept of Environmental Sciences – Botany, Basel Univ., Basel, Switzerland, and Laboratory of Plant Ecology, Faculty of Bioscience Engineering, Ghent Univ., Ghent, Belgium.

Ecography
43: 1386–1399, 2020
doi: 10.1111/ecog.04968

Subject Editor:
Jens-Christian Svenning
Editor-in-Chief: Miguel Araújo
Accepted 11 May 2020

Tree growth is an indicator of tree vitality and its temporal variability is linked to species resilience to environmental changes. Second-order statistics that quantify the cross-scale temporal variability of ecophysiological time series (statistical memory) could provide novel insights into species resilience. Species with high statistical memory in their tree growth may be more affected by disturbances, resulting in lower overall resilience and higher vulnerability to environmental changes. Here, we assessed the statistical memory, as quantified with the decay in standard deviation with increasing time scale, in tree water use and growth of co-occurring European larch *Larix decidua* and Norway spruce *Picea abies* along an elevational gradient in the Swiss Alps using measurements of stem radius changes, sap flow and tree-ring widths. Local-scale interspecific differences between the two conifers were further explored at the European scale using data from the International Tree-Ring Data Bank. Across the analysed elevational gradient, tree water use showed steeper variability decay with increasing time scale than tree growth, with no significant interspecific differences, highlighting stronger statistical memory in tree growth processes. Moreover, Norway spruce displayed slower decay in growth variability with increasing time scale (higher statistical memory) than European larch; a pattern that was also consistent at the European scale. The higher statistical memory in tree growth of Norway spruce in comparison to European larch is indicative of lower resilience of the former in comparison to the latter, and could potentially explain the occurrence of European larch at higher elevations at the Alpine treeline. Single metrics of resilience cannot often summarize the multifaceted aspects of ecosystem functioning, thus, second-order statistics that quantify the strength of statistical memory in ecophysiological time series could complement existing resilience indicators, facilitating the assessment of how environmental changes impact forest growth trajectories and ecosystem services.

Keywords: forest resilience, *Larix decidua* Mill., *Picea abies* (L) Karst., temporal variability, tree hydraulics and growth, tree-ring widths

NORDIC SOCIETY OIKOS

www.ecography.org

© 2020 The Authors. Ecography published by John Wiley & Sons Ltd on behalf of Nordic Society Oikos
This is an open access article under the terms of the Creative Commons Attribution License, which permits use, distribution and reproduction in any medium, provided the original work is properly cited.

Introduction

Tree water use and growth are intrinsically coupled processes that define tree performance and affect terrestrial biogeochemical cycles across spatiotemporal scales. Tree water use and the resulting fluctuations in stem water storage and fluxes, not only shape the terrestrial water cycle through transpiration (a major flux of the terrestrial water budget; Schlesinger and Jasechko 2014, Good et al. 2015), but also affect tree growth (Fatichi et al. 2015, Jensen et al. 2016, Pfautsch 2016, Venturas et al. 2017). Forest growth, apart from direct impact on the terrestrial carbon cycle (Huntzinger et al. 2017, Le Quéré et al. 2018, Fatichi et al. 2019), affects several other biochemical and biophysical processes and trigger local, regional and global scale climate feedbacks (Bonan 2008, Friedlingstein 2015). Quantifying the interplay between tree-level water and carbon dynamics is therefore crucial for better understanding ecosystem responses to future climatic conditions and hydrometeorological extremes (Reichstein et al. 2013, Reyer et al. 2013).

Tree stems serve as 'highways' for water and sugar transport (Furze et al. 2018). Yet, so far, tree water use and growth have primarily been analysed focusing on specific time scales, e.g. diel water use, annual growth. Most of the continuous ecophysiological measurements (e.g. with high frequency sap flow sensors or stem dendrometers) have been performed on relatively short time scales spanning few growing seasons, making it difficult to assess long-term variability in the underlying processes. Tree-ring widths (TRW) provide a long-term perspective of annual tree growth, yet intra-annual growth dynamics remain poorly quantified (Babst et al. 2018). Scrutinizing the variability of ecophysiological processes across a continuum (e.g. hourly to decadal variability) rather than individual time scales (daily, annual, etc.) could shed light on vegetation resilience to environmental changes.

Tree secondary growth, i.e. tissue expansion and meristematic activity leading to stem thickening, is an indicator of tree age and vitality (Dobbertin 2005) and its temporal variability is strongly linked to tree performance, vulnerability and resilience to environmental changes (Lloret et al. 2011, Camarero et al. 2015, Cailleret et al. 2017, Rogers et al. 2018). Tree water storage has been recently suggested as a robust indicator of drought-induced tree mortality risk (e.g. relative tree water content, Martinez-Vilalta et al. 2018). Indeed, similarly to other geophysical phenomena (Mandelbrot and Wallis 1969), the statistical properties of spatiotemporal ecophysiological observations can be used to quantify short- and long-term persistence (statistical memory, hereafter 'memory') of the underlying processes (Pappas et al. 2017) and to infer early-warning signals for critical transitions (Dakos et al. 2012, Scheffer et al. 2015). Power spectra (Kleinen et al. 2003) as well as changes in second-order statistics (Carpenter and Brock 2006) of time series describing ecosystem processes could provide robust indicators of ecological transitions, such as, for example, early-warning signals of drought-induced tree mortality (Camarero et al. 2015, Rogers et al. 2018, Cailleret et al. 2019). Such statistics are widely applied in several disciplines including metrology ('allan deviation graph'; Allan 1966), hydrology (Hosking 1984, Pelletier and Turcotte 1997; and 'climacogram'; Koutsoyiannis 2015), climatology (Mitchell 1976, Koscielny-Bunde et al. 1998, Markonis and Koutsoyiannis 2012) and terrestrial carbon cycle (Katul et al. 2001, Stoy et al. 2005, Mahecha et al. 2007, Paschalis et al. 2015, Pappas et al. 2017), but have not been yet exploited in an ecophysiological context. A systematic characterization of the temporal variability in tree water use and growth across a continuum of time scales could provide important insights not only into tree performance but also into species resilience to environmental changes, as detailed below.

Variability can be intuitively quantified with the estimator of standard deviation of the examined time series ($\hat{\sigma}$). Exploring how $\hat{\sigma}$ decreases with averaging time scale (k), e.g. hourly, daily, seasonal and inter-annual variability (Fig. 1), can reveal the strength of the autocorrelation structure (memory) of the data ('aggregated variance analysis'; Papoulis 1965, Beran 1994, Taqqu et al. 1995, Koutsoyiannis 2015). Applying this approach to ecophysiological time series, species-specific differences in tree water use and growth may be pinpointed and species resilience to environmental stressors may be inferred by the strength of memory in the examined data (Fig. 1; Pappas et al. 2017). The rationale behind this approach is that species which exhibit high variability in ecophysiological variables describing tree vitality (e.g. tree growth) at longer time scales are characterised by a positive autocorrelation structure and display higher memory. Species with higher memory (illustrated, for example, with clusters of local minima or maxima in tree growth time series) may be more affected by disturbances (e.g. atmospheric and soil droughts, insect outbreaks), resulting in lower overall resilience and higher vulnerability to environmental changes (Pappas et al. 2017, van de Leemput et al. 2018). On the other hand, species with steeper variability decay with increasing k correspond to species with lower memory, and thus faster response/recovery in case of disturbances, indicating species with enhanced resilience and lower vulnerability under environmental changes. The emerging patterns of cross-scale variability are the result of whole plant trait coordination with numerous interacting processes that are constrained and coordinated by stoichiometry, resource availability and local environment. As environmental stress persists, e.g. insect outbreaks, repeated or extended periods of water stress, tree vigour gradually decreases till a point that tree mortality is triggered (Rogers et al. 2018). This could be reflected in enhanced autocorrelation in tree ecophysiological time series. Thus, autocorrelation structure of tree ecophysiological time series may provide insights into species resilience, in accordance with previous definitions of ecological resilience (i.e. 'the capacity to reach pre-disturbance performance levels'; Lloret et al. (2011) and references therein), where $\hat{\sigma}$ quantifies the 'deviation' from mean/undisturbed conditions at different time scales.

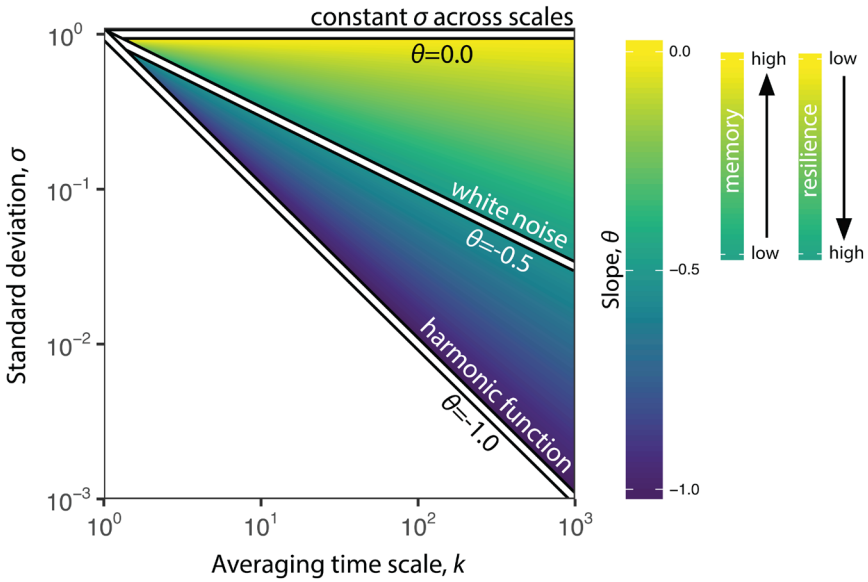


Figure 1. The two-dimensional logarithmic space of standard deviation (σ) versus averaging time scale (k) used for analysing the cross-scale variability and statistical memory in tree water use and growth. Plausible regimes of variability decay are illustrated (coloured area). The variability decay of example processes, namely, deterministic harmonic functions, purely random processes (white noise; no memory) and processes with constant σ across time scales (e.g. random walk, linear trends) are highlighted. A linear slope (θ; [unitless]) was used to approximate the rate of variability decay with increasing k. Slow variability decay with increasing k results in gentle slopes that are indicative of processes with positive autocorrelation structure and memory. Higher memory in tree ecophysiological processes can be a signature of lower species resilience to environmental stressors.

Here, we used the aforementioned approach to analyse tree water use and growth of co-occurring European larch *Larix decidua* and Norway spruce *Picea abies* along a 1400-m elevational gradient in the European Alps (Fig. 2a–b). The dataset consists of measurements of stem radius changes, sap flow and TRW collected using a 'tree-centred' approach (i.e. comprehensive ecophysiological measurements across selected tree individuals; Sass-Klaassen et al. 2016) together with concurrently recorded environmental variables, i.e. air temperature (T), vapour pressure deficit (VPD) and soil moisture. Stem radius changes were partitioned empirically to reversible and irreversible changes and were used to characterize tree water use and growth, respectively. Sap flow and reversible stem radius changes allowed us to quantitatively describe growing-season tree water use from hourly to seasonal time scales. Hourly irreversible stem radius changes and TRW were used to describe tree growth dynamics at seasonal to decadal time scales. Local scale interspecific differences in the tree growth of European larch and Norway spruce across the examined elevational gradient were further investigated at the European scale using TRW from the International Tree-Ring Data Bank (ITRDB, Fig. 2a).

We hypothesize that the cross-scale temporal variability in tree water use will display faster decay in comparison to growth variability decay since tree water use exerts pronounced diurnal fluctuations driven by light and vapour pressure deficit, while tree growth is the result of numerous interacting processes acting across multiple time scales. Moreover, the different growth form of the two conifers, where European larch is deciduous while Norway spruce evergreen species (Ellenberg and Strutt 1988, Lebourgeois et al. 2010), are expected to lead to different signatures of resilience capacity, as a result of their interspecific differences in resource allocation and use.

Material and methods

Study area

The study area is located in the Lötschental region of the Swiss Alps (46°23′40″N, 7°45′35″E; Fig. 2b). The area is mainly covered with well-mixed populations of Norway spruce and European larch distributed along a 1400-m elevational gradient, spanning from 800 m a.s.l. till 2200 m a.s.l. at the treeline and consists of five sampled elevations corresponding to 800, 1300, 1600, 1900 and 2200 m a.s.l. (Fig. 2b, Supplementary material Appendix 1 Table A1). Stand density ranges from ca 605 stems ha^{-1} at low elevations (with 53% Norway spruce and 47% European larch) to ca 207 stems ha^{-1} of only European larch at the treeline (Supplementary material Appendix 1 Table A2; Peters et al. 2017). Environmental conditions were monitored at each sampled elevation including hourly T, relative humidity (Onset, USA, U23-002 Pro; used to calculate VPD) and soil volumetric water content at 10 cm depth (SWC; Decagon, USA, EC-5). A detailed description of the environmental data and their processing is provided in Peters et al. (2018a, b). Long-term mean annual total precipitation in the valley exceeds 800 mm while mean

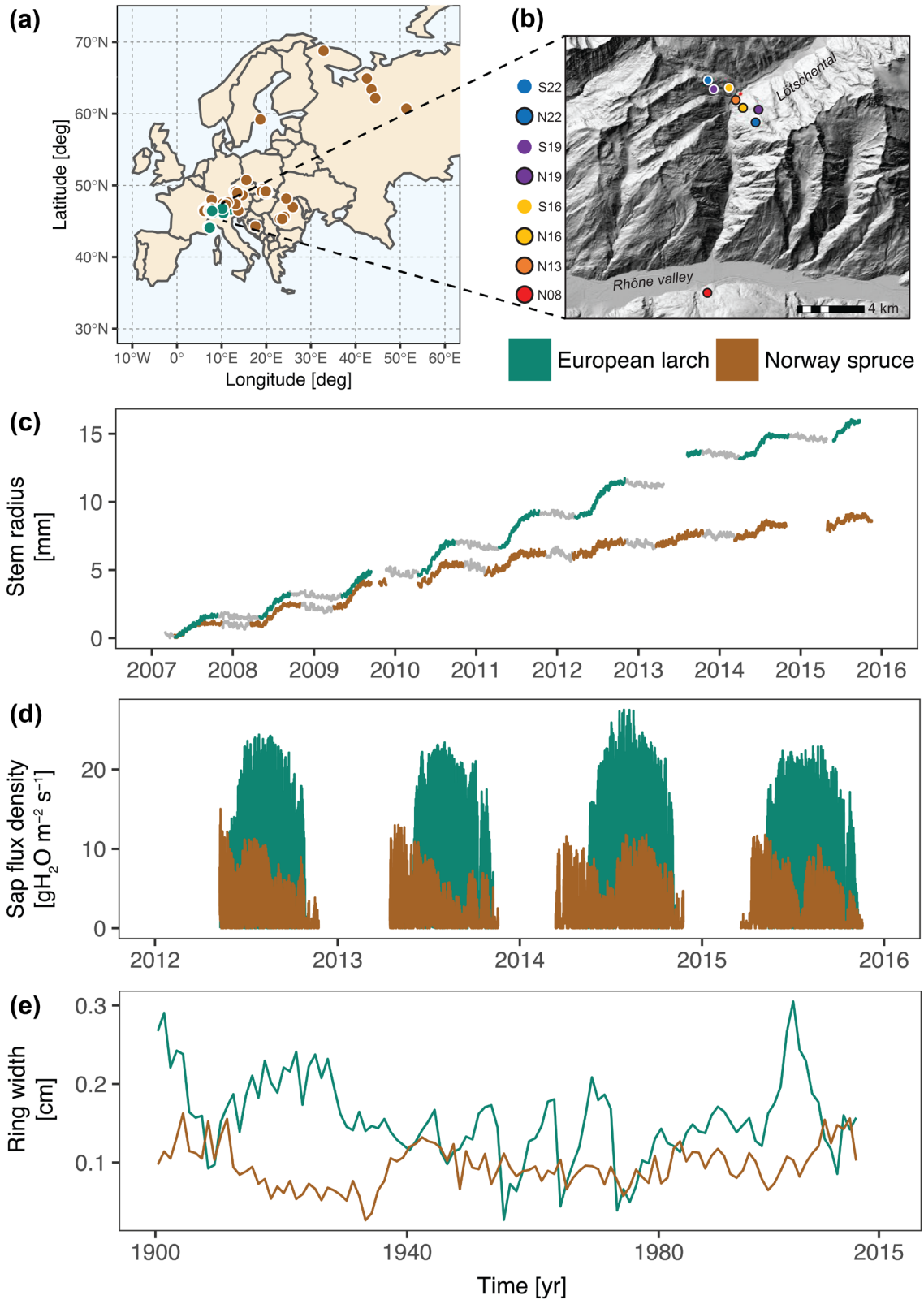


Figure 2. (a) Spatial distribution of the analysed tree-ring widths from ITRDB and (b) the Lötschental region of the Swiss Alps where measurements of tree water use and growth for European larch and Norway spruce are available. Example time series of the variables used to describe tree water use and growth are also depicted, namely, (c) hourly stem radius changes (coloured lines correspond to the growing seasons), (d) hourly sap flux density and (e) annual tree-ring widths. Data correspond to example trees at 1600 m a.s.l.

annual T approximates 5°C. Mean growing season T (May–October from 2008 to 2015; $\bar{T}_{GS}$) ranges from 15.4°C at 800 m a.s.l. to 8.0°C at the treeline (King et al. 2013). The treeline coincides with the distribution limit of European larch while the distribution limit of Norway spruce occurs at 1900 m a.s.l., where meteorological conditions are slightly milder (i.e. $\bar{T}_{GS} \sim 8.9$°C).

Stem radius changes

High-precision point dendrometers (DR Ecomatik, Munich, Germany) were used to monitor stem radius changes of mature European larch and Norway spruce along the elevational gradient covering north- and south-facing slopes. Data was recorded on a 15-min to hourly resolution using a CR1000 data logger (Campbell Scientific, Logan, UT, USA) and corrections were applied to account for thermal effects following the manufacturer's specifications. Data were averaged to an hourly resolution to provide consistent time steps across all individuals. A detailed description of the experimental design, instrumentation and data pre-processing is provided in King et al. (2013). Here, we used hourly stem radius data during nine growing seasons (2007–2015) from fifteen European larch and twelve Norway spruce distributed across the study area (Fig. 2c, Supplementary material Appendix 1 Table A1, Fig. A1–A7). Start and end of the growing season for each year was defined by the first and last observation of the typical transpiration cycle characterized by positive sinusoidal stem radius fluctuations, with highest values in the early morning (08:00–10:00 GMT) and lowest in the late afternoon (16:00–18:00 GMT; Fig. 2b).

Stem radius at time t_i [h], denoted as $R_{H|t_i}$ [mm], where i indicates a specific hour of the day, was partitioned empirically to 1) irreversible changes (expansion) in the stem radius as a result of tree growth ($G^{SRF}_{H|t_i}$; [µm]) and 2) reversible stem radius changes due to tree water use ($W^{SRF}_{H|t_i}$; [µm]), i.e. sub-daily variation in stem water storage (Fig. 3a–d). The former was estimated as $G^{SRF}_{H|t_i} = g_{H|t_i} - g_{H|t_{i-1}}$ where $g_{H|t_i}$ was defined according to Zweifel et al. (2016), i.e.

$$g_{H|t_i} = \begin{cases} R_{H|t_i} - \max\left(R_{H|t<t_i}\right), \text{when } R_{H|t_i} \geq \max\left(R_{H|t<t_i}\right) \\ 0, \text{when } R_{H|t_i} < \max\left(R_{H|t<t_i}\right) \end{cases} \quad (1)$$

The latter was estimated as the deviation of $R_{H|t_i}$ from its daily mean, R_D [mm], i.e.

$$W^{SRF}_{H|t_i} = R_{H|t_i} - R_D \quad (2)$$

assuming that at the sub-daily time scales $R_{H|t_i}$ variability was closer related to tree water use than growth (Fig. 3c–d; King et al. 2013, Pappas et al. 2018). It is worth highlighting that, complementing the aforementioned empirical approach, recent literature provides methods for process-based partitioning of high frequency stem radius fluctuations to hydraulic-, osmotic- and growth-driven changes (Mencuccini et al. 2013, 2017, Chan et al. 2016) with previous method intercomparison showing comparable results between the derived growth signals (Eller et al. 2018).

Sap flow

Sap flux density (J_s; [$gH_2O\,m^{-2}\,s^{-1}$]) of twelve European larch and nine Norway spruce, distributed across the study area was measured from April 2012 to October 2015 (Fig. 2d, Supplementary material Appendix 1 Table A1, Fig. A8–A11). Thermal dissipation probes (20-mm long stainless steel probes, with a 2-mm diameter; Tesaf, Univ. of Padova, Italy) were used (Granier 1987, Lu et al. 2004) and data were stored with a 15-min resolution on a CR1000 data logger (Campbell Scientific, Logan, UT, USA). Data were aggregated to hourly resolution. The values of J_s were calculated using species-specific calibration curves established with cut-stem calibration method for the two species according to Steppe et al. (2010). For further details on data processing see Peters et al. (2018a, b). We characterized tree water use using the first-order derivative of hourly sap flux density, i.e. $W^{SFD}_{H|t} = \Delta J_S / \Delta t$; [$gH_2O\,m^{-2}$], a proxy of tree hydraulic functioning comparable to the information derived from the stem dendrometers ($W^{SRF}_{H|t_i}$; Fig. 3e–g).

Tree-ring widths

Tree-ring widths from European larch and Norway spruce were collected at all sampled elevations and were used to describe their inter-annual growth dynamics (G^{TRW}_Y [cm]). We analysed 92 and 70 trees from European larch and Norway spruce, respectively, that were sampled at breast height (~1.3 m above ground) with increment borers (Haglöf, Sweden; Supplementary material Appendix 1 Table A1). Standard dendrochronological techniques were used to prepare the samples, measure ring widths and cross-date visually and statistically, as detailed in Peters et al. (2017). In order to account for age and size effects in TRW, instead of detrending the TRW time series with predefined filters (Peters et al. 2015, Brienen et al. 2017), we discarded the first 30 yr of each TRW time series, and consistently use data from 1900 to 2011 for all the sampled tree cores (Supplementary material Appendix 1 Fig. A12). This approach was preferred since it prevents unrealistic reduction of the variance in the original data due to data detrending, yet potential age-related trends in the TRW time series during the period 1900–2011 cannot be eliminated with certainty. It is worth highlighting that strong reductions in TRW for European larch at the study area, occurring with a regular 9-yr cycle (Fig. 2e, Supplementary material Appendix 1 Fig. A12), are caused by the larch budmoth (*Zeiraphera diniana* Guénée) outbreaks severely defoliating its host (Esper et al. 2007).

To further analyse species-specific growth dynamics at the regional scale, we used publicly available TRW data across Europe, obtained from the International Tree-Ring Data Bank (ITRDB, Fig. 2a; <www.ncdc.noaa.gov/data-access/paleoclimatology-data/datasets/tree-ring>). We isolated all

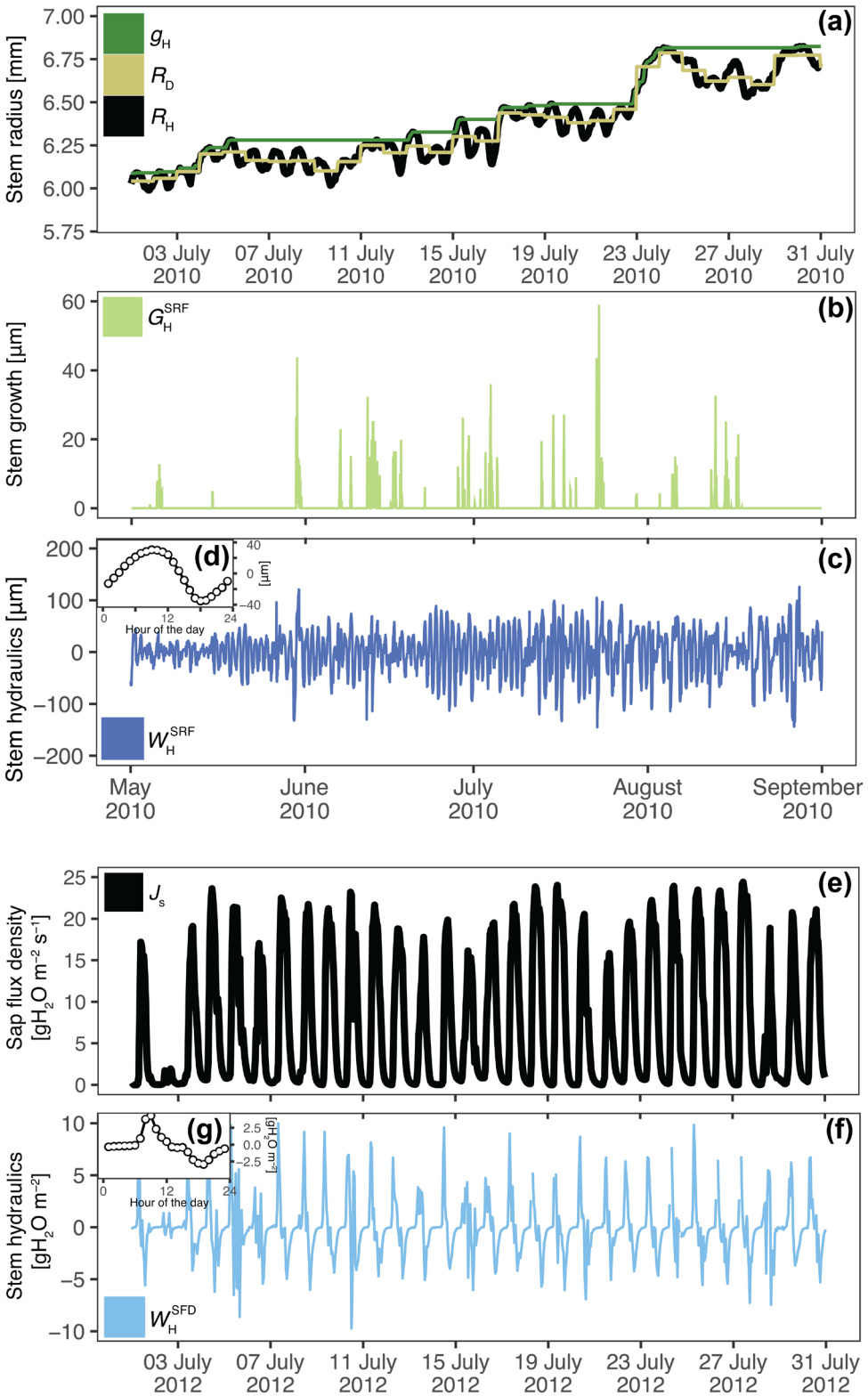


Figure 3. Overview of the dendrometer-derived tree growth as well as the dendrometer- and sap-flow-derived tree water use for an example European larch at 1600 m a.s.l. (a) Hourly and mean daily stem radius, R_H and R_D, respectively, as well as hourly stem increase due to tree growth (g_H; Eq. 1) during July 2010. (b) Hourly dendrometer-derived tree growth (G_H^{SRF}) and (c) tree water use (W_H^{SRF}; Eq. 2) from May to September 2010 and (d) the corresponding diurnal cycle of W_H^{SRF}. (e) Hourly sap flux density during July 2012, (f) sap-flow-derived tree water use (W_H^{SFD}) and (g) the resulting growing-season (May–August 2012) diurnal cycle of W_H^{SFD}.

individual TRW time series from the ITRDB for European larch (species code 'LADE', 26 sites) and Norway spruce (species codes 'PCAB', 85 sites) which contained at least 150 tree rings. Subsequently, we removed the first 50 yr of the series, to reduce the age effect, and clipped the data to the common period of 1880–1980. A larger time window than the TRW from Lötschental was selected for addressing the age effect in the ITRDB dataset since we have no information on stand history and subsequent age trends within these sites. This resulted in a total of 593 and 1250 TRW time series covering elevations from 900 to 2231 and 35 to 2065 m a.s.l. for European larch and Norway spruce, respectively.

Cross-scale temporal variability

Cross-scale temporal variability in major environmental variables (i.e. T, VPD, SWC) as well as tree water use and growth was quantified by analysing how the empirical standard deviation ($\hat{\sigma}$) of the examined variable changes across different averaging time scales (k; Fig. 1). This offers an intuitive framework for investigating second-order statistics of the underlying processes and for quantifying the strength of memory (long-term persistence) (Koutsoyiannis 2015). The values of k range from the original temporal resolution (Δ) of each dataset, i.e. one hour for environmental, sap flow and dendrometer data and one year for TRW, to $L/10$, where L is the total length of the time series, resulting in robust estimation of $\hat{\sigma}$ at $k = L/10$ with at least ten values (Koutsoyiannis 2015). In order to facilitate comparisons between species and variables, data were standardized, i.e. zero mean and unit variance, at their original time scale.

A quantitative assessment of the observed patterns in cross-scale variability was conducted by approximating the observed variability decay with a linear slope (θ [unitless]; Fig. 1). The values of θ (< 0 for decreasing slopes) are equal to $H-1$, where H denotes the Hurst coefficient (Hurst 1951), a measure of long-term persistence ('aggregated variance analysis'; Papoulis 1965, Beran 1994, Taqqu et al. 1995, Koutsoyiannis 2015). The values of θ were estimated per individual tree for each analysed variable (or per sampled elevation for the meteorological variables) using the linear part of variability decay, i.e. for time scales ≥ 24 h. The estimated values of θ were then compared with theoretical slopes from characteristic deterministic and stochastic processes. This included harmonic functions with constant periodicity ($\theta_{HR} = -1.0$, Fig. 1; Markonis and Koutsoyiannis 2012, Pappas et al. 2017) or purely random processes like white noise (i.e. no memory; $\theta_{WN} = -0.5$, Fig. 1; Koutsoyiannis 2015). When $\theta \in (-1.0, -0.5)$ the underlying process is antipersistent with irregular periodicity. For $\theta \in (-0.5, 0)$ the underlying process is characterized by a positive autocorrelation structure (i.e. short- or long-term persistence) and the larger the value of θ the higher the memory of the underlying process (Fig. 1). All analyses were conducted in R ver. 3.6.0 (R Core Team).

Results

Cross-scale variability in tree water use

The variability decay in tree water use, as quantified with the first-order derivative of sap flux density, W_H^{SFD} and stem radius changes, W_H^{SRF}, showed similar patterns as we move from hourly to seasonal time scales (Fig. 4–6). W_H^{SFD} and W_H^{SRF} cross-scale variability showed steep decrease with increasing time scale. An increase in time scale by one order of magnitude resulted approximately in an equivalent decrease in the standard deviation of W_H^{SFD} and W_H^{SRF}. Moreover, substantial drops in standard deviation occurred at characteristic time scales corresponding to $\tau = 24$ h and $m\tau/2$, where $m \in \mathbb{N}$ (Fig. 4). This pattern of variability decay was the result of the pronounced harmonic fluctuations (i.e. sinusoidal cycle with periodicity $\tau = 24$ h; Pappas et al. 2017) in tree hydraulic functioning (Fig. 3d, g) and was consistent for both species across the study area from lower to higher elevations (Fig. 5). Growing season diurnal fluctuations in W_H^{SRF} (Fig. 3d) and W_H^{SFD} (Fig. 3g) showed a consistent sinusoidal pattern: during night-time there was an increase in stem radius and water storage, as a result of lower VPD and transpiration rates; during day-time there was a decrease in stem radius and depletion of stem water storage as result of higher transpiration rates and atmospheric demand in comparison to root water supply (Zweifel et al. 2001, King et al. 2013, Pappas et al. 2018). Therefore, across all the instrumented trees at the study area, the slope of variability decay with time scale (throughout the text values corresponds to mean ± one standard deviation) for W_H^{SFD} ($\theta_W^{SFD} = -0.98 \pm 0.01$ for European larch; $\theta_W^{SFD} = -1.03 \pm 0.02$, for Norway spruce) and W_H^{SRF} ($\theta_W^{SRF} = -0.97 \pm 0.01$ for European larch; $\theta_W^{SRF} = -0.98 \pm 0.01$ for Norway spruce) approximated the theoretical slope of an harmonic function with constant periodicity ($\theta_{HR} = -1.00$; Fig. 6a). The variability decay of tree water use, shaped by the pronounced harmonic fluctuations, falls outside the meteorological envelope of variability as defined by T, SWC and VPD (Supplementary material Appendix 2 Fig. A13). The slope of variability decay of T is mild and well-constrained across elevations ($\theta_T = -0.04 \pm 0.01$; Supplementary material Appendix 2 Fig. A13), while the slope of variability decay of VPD is steeper and becomes more negative with increasing elevation ($\theta_{VPD} = -0.18 \pm 0.07$; Supplementary material Appendix 2 Fig. A13). The pattern of variability decay of SWC is more complex as we move from low to high elevations ($\theta_{SWC} = -0.17 \pm 0.06$; Supplementary material Appendix 2 Fig. A13), most probably due to topographic effects and hysteretic behaviour of SWC dynamics (Fatichi et al. 2015). The time series length of the available dendrometer and sap flow data did not allow us to characterize inter-annual time scales. No significant interspecific differences were found in the variability decay patterns of tree water use between European larch and Norway spruce (t-test; p-value > 0.05 for θ_W^{SFD} and θ_W^{SRF}; Supplementary material

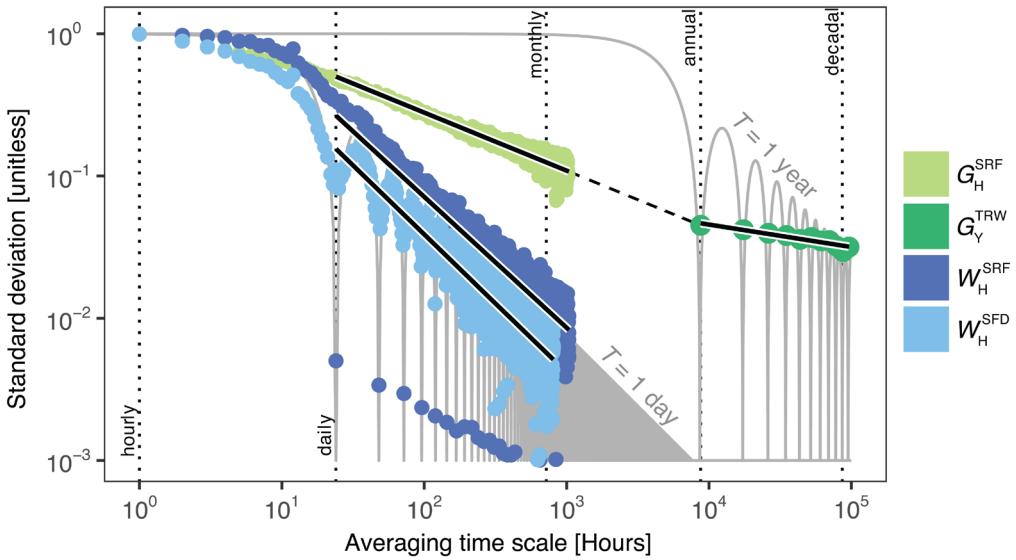


Figure 4. Cross-scale temporal variability of tree water use and growth and the estimated slopes used to approximate their variability decay patterns, for an example European larch at 1600 m a.s.l. Dotted vertical lines highlight characteristic time scales. Solid grey lines depict the theoretical variability decay of harmonic functions with constant periodicities equal to one day and one year. Coloured points depict the standard deviation of the process of interest at various averaging time scales. Tree growth was quantified with hourly irreversible stem radius changes (G_H^{SRF}) and annual tree-ring widths (G_Y^{TRW}) while tree water use with dendrometer- (W_H^{SRF}) and sap-flow-based estimates (W_H^{SFD}). All variables with hourly temporal resolution (i.e. G_H^{SRF}, W_H^{SRF} and W_H^{SFD}) were standardized (i.e. zero mean and unit variance) at the hourly time scale. Tree-ring widths have an annual time step, thus, for illustration purposes, the standard deviation of G_Y^{TRW} was linearly transformed so that at the annual time scale it matches with the standard deviation of G_H^{SRF}. For each of the analysed variables a linear model was fitted for time scales ≥ 24 h to quantify the slope of the decrease in standard deviation with increasing time scale (solid black lines). Note that the time series length of the dendrometer data does not allow for robust estimations of the G_H^{SRF} standard deviation at the annual time scale, thus, a linear model was fitted to describe the decay in standard deviation with time scale (solid black line) and used to predict its value at the annual time scale (dashed black line).

Appendix 1 Table A1, Fig. 6a), while the Pearson's correlation coefficients (r) of θ_W^{SFD} and θ_W^{SRF} with elevation were also weak and non-significant for both species (p-values > 0.05; Supplementary material Appendix 1 Table A1, Fig. 5).

Cross-scale variability in tree growth

Irreversible stem radius changes in European larch and Norway spruce were used to characterize the continuum of variability in tree growth from hourly to seasonal time scales (G_H^{SRF}). Annual tree-ring widths (G_Y^{TRW}) were used to extend the continuum of tree growth variability and capture inter-annual to decadal time scales. For both European larch and Norway spruce, the variability of G_H^{SRF} and G_Y^{TRW} showed a gentle decrease with increasing time scale (Fig. 4). The slopes of the variability decay in G_H^{SRF} and G_Y^{TRW} were shallower than the theoretically expected slope for a purely random process (i.e. white noise; $\theta_{WN} = -0.50$) with the slopes of G_H^{SRF} being relatively steeper in comparison to those of G_Y^{TRW} (i.e. $\theta_G^{SRF} = -0.34 \pm 0.08$ and $\theta_G^{TRW} = -0.18 \pm 0.08$ for European larch; $\theta_G^{SRF} = -0.28 \pm 0.06$ and $\theta_G^{TRW} = -0.10 \pm 0.05$ for Norway spruce; Fig. 4–6). Meteorological conditions frame an envelope for tree-ring derived growth variability, with θ_G^{TRW} for Norway spruce approaching the variability decay of T ($\theta_T = -0.04 \pm 0.01$; upper boundary) and the slopes of variability decay of SWC ($\theta_{SWC} = -0.17 \pm 0.06$) and VPD ($\theta_{VPD} = -0.18 \pm 0.07$) being closer to θ_G^{TRW} of European larch (Supplementary material Appendix 2 Fig. A13).

Interspecific differences in the tree growth variability decay for European larch and Norway spruce were found to be significant (t-test; p-value < 0.05; Supplementary material Appendix 1 Table A1) based on both G_H^{SRF} and G_Y^{TRW} data (Fig. 6b). The growth dynamics of European larch displayed steeper slopes in the cross-scale variability continuum (i.e. lower memory, higher resilience; Fig. 1) in comparison to Norway spruce that showed shallower slopes (i.e. higher memory, lower resilience; Fig. 1). Such interspecific differences were consistent across the study area including European larch and Norway spruce from lower and higher elevations (Fig. 5b). The correlations between θ_G^{SRF} and elevation were weak and non-significant for both species (p-values > 0.05), while θ_G^{TRW} was weakly correlated with elevation at low significance level, i.e. $r = 0.21$ (p-value = 0.05) and $r = 0.29$ (p-value = 0.01) for European larch and Norway spruce, respectively (Supplementary material Appendix 1 Table A1, Fig. 5).

The regional-scale analysis of the TRW data for European larch and Norway spruce, revealed similar patterns in the growth variability decay of the two species

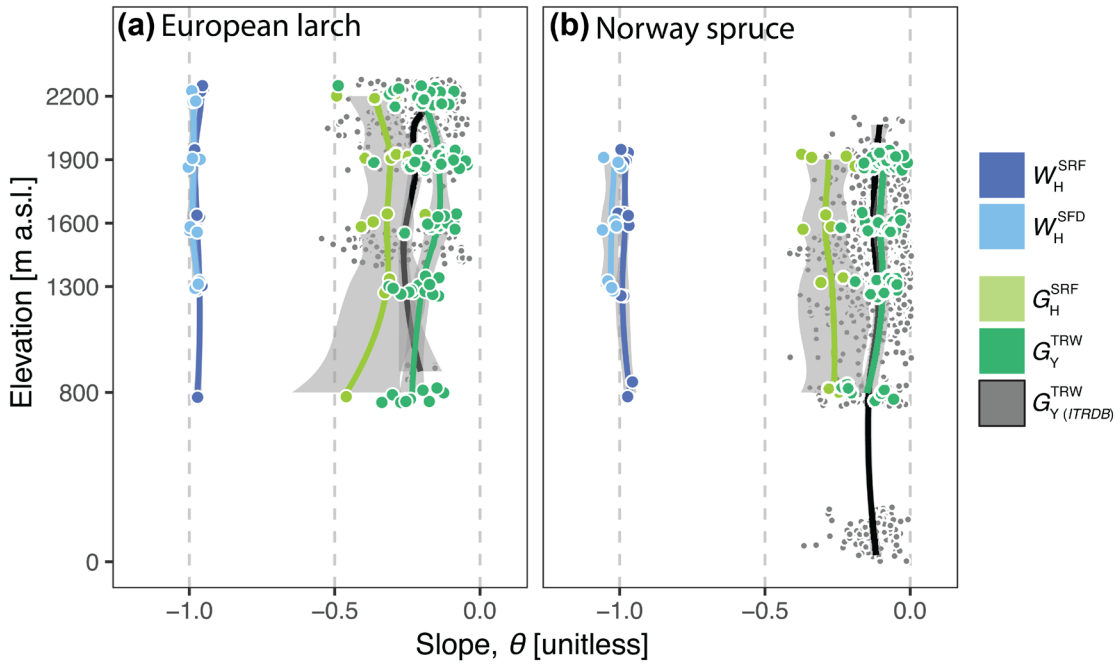


Figure 5. Distribution of the slopes (θ; [unitless]) of the decay in standard deviation with averaging time scale across elevations for tree water use (W_H^{SRF} and W_H^{SFD}, for dendrometer- and sap-flow-based estimates, respectively) and growth (G_H^{SRF} and G_Y^{TRW}, for dendrometer- and ring-width-derived growth, respectively) for (a) European larch and (b) Norway spruce at the Lötschental valley. Coloured points correspond to different variables while solid coloured lines to *loess* smoothing for each variable across elevations (standard errors are depicted in light grey). Grey dots and solid black lines depict the estimated θ values from the tree-ring data across Europe from the ITRDB for the two species ($G_{Y(ITRDB)}^{TRW}$). For enhancing figure's clarity data points are spread around each elevation (± 50 m).

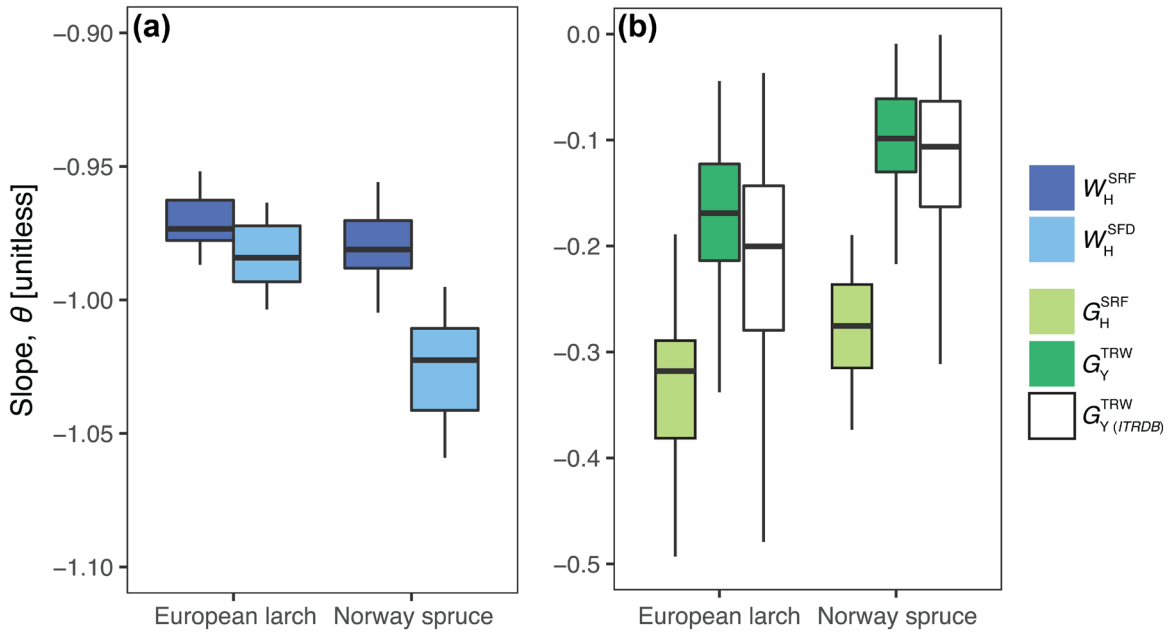


Figure 6. Distribution of the slopes (θ; [unitless]) of the decay in standard deviation with averaging time scale for (a) tree water use (W_H^{SRF} and W_H^{SFD}, for dendrometer- and sap-flow-based estimates, respectively) and (b) tree growth (G_H^{SRF} and G_Y^{TRW}, for dendrometer- and ring-width-derived growth, respectively) for European larch and Norway spruce at the Lötschental valley, as well as θ values from the tree-ring data across Europe from the ITRDB for the two species ($G_{Y(ITRDB)}^{TRW}$). Note the different value range in the y-axes of the two subplots.

across Europe ($\theta^{TRW}_{G(ITRDB)}$) as in the Lötschental region. The interspecific differences in $\theta^{TRW}_{G(ITRDB)}$ were significant, i.e. $\theta^{TRW}_{G(ITRDB)} = -0.22 \pm 0.10$ and $\theta^{TRW}_{G(ITRDB)} = -0.12 \pm 0.08$, for European larch and Norway spruce, respectively (t-test; p-value < 0.05; Fig. 6), while the correlation between $\theta^{TRW}_{G(ITRDB)}$ and elevation for both species was weak, i.e. $r = 0.24$ (p-value < 0.05) for European larch and $r = 0.05$ (p-value = 0.09) for Norway spruce (Supplementary material Appendix 1 Table A1, Fig. 5). Tree age, inferred here from the number of recorded tree rings, changed between species and across elevations for the data from Lötschental and ITRDB. Yet, the correlations between the estimated slopes of growth variability decay and tree age were found to be weak with low significance (Supplementary material Appendix 3 Fig. A14).

Discussion

Contrasting patterns of cross-scale temporal variability in tree water use and growth

While tree water use and growth are intrinsically coupled processes (Fatichi et al. 2015, Steppe et al. 2015, Venturas et al. 2017) our analysis revealed that their temporal variability exhibits different decay patterns as we move from short- to longer time scales. Across the study area and for both European larch and Norway spruce, the variability in tree water use decreased rapidly with time scale. The mechanism behind this pattern is the pronounced diurnal fluctuations triggered by light and the leaf-to-air vapour pressure gradient (Damour et al. 2010, Venturas et al. 2017). While daily water use of the two conifers has been found to be comparable, their diurnal temporal dynamics can differ significantly (Schulze et al. 1985). European larch and Norway spruce display different stomatal regulation strategies (Anfodillo et al. 1998, Obojes et al. 2018, Peters et al. 2018a) that can affect carbon assimilation and growth across multiple time scales, as detailed below.

Contrary to tree water use, the temporal variability of tree growth decreased more gently as we move from short to longer time scales, underlining the importance of lagged effects in tree-level resource allocation and remobilization (Anderegg et al. 2015, Ogle et al. 2015, Pappas et al. 2017, Huang et al. 2018). The phenology of tree organs, such as fine roots, cambium, non-structural carbohydrates (NSC) and leaves, as well as their coordination and response to prevailing environmental conditions, shape plants' resource acquisition and growth across a continuum of time scales (Delpierre et al. 2016a). At the intra-annual time scales, wood formation processes (i.e. xylogenesis) and the resulting biomass production, have been found to be in asynchrony with the associated xylem size increase resulting in monthly or longer time lags (Cuny et al. 2015, Castagneri et al. 2017). Seasonal dynamics of NSC have been found to play a dual role in tree growth, being an active storage for immediate plant functions (i.e. affecting intra-annual time scales), but also being a passive reservoir for future use (i.e. affecting inter-annual time scales) (Richardson et al. 2013, Simard et al. 2013, Dietze et al. 2014, Hartmann and Trumbore, 2016, Martinez-Vilalta et al. 2016). Moreover, wood phenology (carbon sink) could play a more important role in shaping inter-annual tree growth in comparison to photosynthetic production (carbon source) (Körner, 2013, Delpierre et al. 2016b). At the inter-annual time scales, carry over effects of spring or autumn anomalies in forest productivity have been reported at the ecosystem level with eddy covariance measurements of net ecosystem exchange between the land surface and the atmosphere (Richardson et al. 2010, Wu et al. 2013). It is thus the interplay of numerous processes that affect tree growth across a continuum of time scales (e.g. photosynthesis, meristematic activity, phenology, NSC dynamics). In accordance with previous findings at the ecosystem level, cross-scale variability in meteorological conditions envelopes variability of carbon fluxes and tree growth, where energy and temperature define the upper limit and water availability (e.g. precipitation, SWC, VPD) the lower limit of the variability envelope (Pappas et al. 2017).

The estimated tree growth variability decay with dendrometer data showed relatively steeper slopes in comparison to those estimated with tree rings. This highlights that empirically deriving intra-annual tree growth solely from dendrometer data remains uncertain (Deslauriers et al. 2007, De Swaef et al. 2015). The pronounced diurnal stem shrinkage and swelling due to tree water use could mask the intra-annual irreversible stem radius changes due to cambial growth (e.g. cell division and expansion; Chan et al. 2016) and may lead to underestimation of the intra-annual variability in tree growth processes. Thus, complementing the empirical partitioning of growth and hydraulic signals presented here, a process-based partitioning of dendrometer data, where bark thickness changes are mechanistically attributed to tree hydraulics (i.e. water potential-induced changes), osmotic-induced changes and irreversible growth, is expected to shed light into the interplay of growth and water-use variability at sub-annual time scales (Mencuccini et al. 2013, 2017, Chan et al. 2016, Eller et al. 2018). Sub-monthly time series of xylem anatomical features (Fonti et al. 2010, von Arx and Carrer 2014) could be also incorporated in the proposed approach to better characterize the continuum of tree growth variability at the intra-annual time scales, and confront the growth patterns derived from stem dendrometers.

Cross-scale temporal variability in tree growth and species resilience

While the cross-scale variability in tree water use did not show interspecific differences, their cross-scale tree growth variability differed significantly with the growth dynamics of European larch having faster variability decay (lower memory) in comparison to Norway spruce (Fig. 6). This pattern is consistent for tree growth estimates derived from

dendrometer data and TRW at the Lötschental region, as well as from TRW for the two species across Europe and confirms the higher resilience to environmental stressors of European larch in comparison to Norway spruce that is reported in literature. Our analysis revealed no clear dependences of the slope of the variability decay in tree growth with elevation, neither at the local (Lötschental valley of the Swiss Alps) nor at the regional scale (ITRDB across Europe). Uncertainties associated with the slope estimates of variability decay (i.e. linear approximation, time-series length, age and size effects in ring widths), as well as confounding factors that may change with elevation (e.g. *T* and precipitation cross-correlations as well as species competition) could explain this lack of elevational dependence.

In accordance with observational evidence from other mountain forests in the European Alps, our analysis indicates that European larch is likely more resilient and less vulnerable to environmental changes in comparison to Norway spruce, potentially explaining the occurrence of the former in higher elevations at the Alpine treeline. The enhanced resilience capacity of European larch, as quantified here with the strength of the statistical memory in tree growth time series, is also demonstrated by its recovery from larch budmoth outbreaks, occurring across the examined elevational gradient during the second half of 20th century at a regular 9-yr cycle (Fig. 2e, Supplementary material Appendix 1 Fig. A12; Esper et al. 2007). A multi-species analysis of tree rings from Alpine mountain forests in the northern Limestone Alps, southeast Germany, confirmed these findings based on mean growth rates, climatic sensitivities and lag-1 autocorrelations of Norway spruce to changing climatic conditions (e.g. higher temperature and water limitations) in comparison to European larch (Hartl-Meier et al. 2014). In addition, Lévesque et al. (2013) using dendroecological methods quantified the higher drought sensitivity of Norway spruce radial growth to climatic conditions in comparison to other conifers from the European Alps, including European larch. A recent analysis of sap flow and dendrometer data from European larch along an elevational gradient at the southern Tyrol, Italy, demonstrated the enhanced plasticity and adaptability of larch to climatic condition and its potential upward shift under future climates (Obojes et al. 2018). This plastic behaviour of European larch to changing environmental conditions is confirmed at our study site at the Lötschental region by the higher plasticity of European larch stomatal conductance to temperature changes in comparison to Norway spruce (Peters et al. 2018a).

Broader implications

Robust quantification of the vulnerability and resilience of forested ecosystems to environmental changes is essential for better understanding how climate change affects tree performance and mortality (Allen et al. 2015, Hartmann et al. 2018) as well as for assessing climate change impacts on forest health (Trumbore et al. 2015) and ecosystem services (Theurillat and Guisan 2001, Elkin et al. 2013). Traditionally, the vulnerability of forested ecosystems has been quantified by analysing how vegetation response, described, for example, with individual TRW time series or TRW chronologies, changes with environmental conditions, such as temperature and soil water availability (Lloret et al. 2011, Lévesque et al. 2013, Fang and Zhang 2018, Serra-Maluquer et al. 2018). Recently, temporal dynamics of tree- and landscape-level ecophysiological variables describing vegetation growth have been found to provide new insights into drought-induced tree mortality and were used to reveal early-warning signals of such type of disturbances (Camarero et al. 2015, Cailleret et al. 2017, 2019, Rogers et al. 2018). Since single metrics of resilience cannot often summarize the multifaceted aspects of ecosystem functioning, second-order statistics that quantify the strength of statistical memory in tree ecophysiological time series could complement these efforts and link species performance and species resilience to environmental changes. A quantitative description of resilience capacity could be used to infer species vulnerability to environmental stressors and, ultimately, mortality risk. This approach could be used to scrutinize global networks of tree ecophysiological data such as for example TRW (e.g. ITRDB) and sap flow (e.g. SAPFLUXNET; <http://sapfluxnet.creaf.cat/>). Such information could provide quantitative insights into species-specific sensitivities facilitating thus adaptive forest management under environmental changes.

Data availability statement

The R code used in the presented analysis is available from: <https://github.com/PappasChristoforos/alps_variability_decay>. Data from the Lötschental valley used in this study are available upon request from the corresponding author and will be archived at <www.envidat.ch/>.

Acknowledgements – We would like to thank David C. Frank, Flurin Babst, Greg King and Stefan Klesse for their help with data collection at the Lötschental valley. Stefan Klesse, Miguel Mahecha and Yannis Markonis are acknowledged for fruitful discussions and detailed feedback on an earlier version of the manuscript.
Funding – CP and RLP acknowledge the support of the Swiss National Science Foundation, SNF, Grant P300P2_174477 and P2BSP3_184475, respectively. Data collection was performed in the framework of the SNF projects INTEGRAL (121859) and LOTFOR (150205).
Author contributions – CP designed the study with input from RLP and PF. RLP and PF collected, processed and provided the dendrometer, sap flow and tree-ring width data. CP conducted the analyses and wrote the manuscript. All authors contributed in editing the manuscript.

References

Allan, D. 1966. Statistics of atomic frequency standards. – Proc. IEEE 54: 221–230.

Allen, C. D. et al. 2015. On underestimation of global vulnerability to tree mortality and forest die-off from hotter drought in the Anthropocene. – Ecosphere 6: art129.
Anderegg, W. R. L. et al. 2015. Pervasive drought legacies in forest ecosystems and their implications for carbon cycle models. – Science 349: 528–532.
Anfodillo, T. et al. 1998. Tree water relations and climatic variations at the alpine timberline: sesonal changes of sap flux and xylem water potential in *Larix decidua*, *Picea abies* and *Pinus cembra*. – Ann. Sci. For. 55: 159–172.
Babst, F. et al. 2018. When tree rings go global: challenges and opportunities for retro- and prospective insight. – Quat. Sci. Rev. 197: 1–20.
Beran, J. 1994. Statistics for long-memory processes. – Chapman and Hall.
Bonan, G. B. 2008. Forests and climate change: forcings, feedbacks and the climate benefits of forests. – Science 320: 1444–1449.
Brienen, R. J. W. et al. 2017. Tree demography dominates long-term growth trends inferred from tree rings. – Global Change Biol. 23: 474–484.
Cailleret, M. et al. 2017. A synthesis of radial growth patterns preceding tree mortality. – Global Change Biol. 23: 1675–1690.
Cailleret, M. et al. 2019. Early-warning signals of individual tree mortality based on annual radial growth. – Front. Plant Sci. 9: 1–14.
Camarero, J. J. et al. 2015. To die or not to die: early warnings of tree dieback in response to a severe drought. – J. Ecol. 103: 44–57.
Carpenter, S. R. and Brock, W. A. 2006. Rising variance: a leading indicator of ecological transition. – Ecol. Lett. 9: 308–315.
Castagneri, D. et al. 2017. How does climate influence xylem morphogenesis over the growing season? Insights from long-term intra-ring anatomy in *Picea abies*. – Ann. Bot. 119: 1011–1020.
Chan, T. et al. 2016. Separating water-potential induced swelling and shrinking from measured radial stem variations reveals a cambial growth and osmotic concentration signal. – Plant Cell Environ. 39: 233–244.
Cuny, H. E. et al. 2015. Woody biomass production lags stem-girth increase by over one month in coniferous forests. – Nat. Plants 1: 15160.
Dakos, V. et al. 2012. Robustness of variance and autocorrelation as indicators of critical slowing down. – Ecology 93: 264–271.
Damour, G. et al. 2010. An overview of models of stomatal conductance at the leaf level. – Plant. Cell Environ. 33: 1419–38.
De Swaef, T. et al. 2015. Stem diameter variations as a versatile research tool in ecophysiology. – Tree Physiol. 35: 1047–1061.
Delpierre, N. et al. 2016a. Temperate and boreal forest tree phenology: from organ-scale processes to terrestrial ecosystem models. – Ann. For. Sci. 73: 5–25.
Delpierre, N. et al. 2016b. Wood phenology, not carbon input, controls the interannual variability of wood growth in a temperate oak forest. – New Phytol. 210: 459–470.
Deslauriers, A. et al. 2007. Dendrometer and intra-annual tree growth: what kind of information can be inferred? – Dendrochronologia 25: 113–124.
Dietze, M. C. et al. 2014. Nonstructural carbon in woody plants. – Annu. Rev. Plant Biol. 65: 667–687.
Dobbertin, M. 2005. Tree growth as indicator of tree vitality and of tree reaction to environmental stress: a review. – Eur. J. For. Res. 124: 319–333.
Elkin, C. et al. 2013. A 2°C warmer world is not safe for ecosystem services in the European Alps. – Global Change Biol. 19: 1827–1840.
Ellenberg, H. H. and Strutt, G. K. 1988. Vegetation ecology of Central Europe. – Cambridge Univ. Press.
Eller, C. et al. 2018. Xylem hydraulic safety and construction costs determine tropical tree growth. – Plant Cell Environ. 41: 548–562.
Esper, J. et al. 2007. 1200 Years of regular outbreaks in alpine insects. – Proc. R. Soc. B 274: 671–679.
Fang, O. and Zhang, Q. 2018. Tree resilience to drought increases in the Tibetan Plateau. – Global Change Biol. 25: 245–253.
Fatichi, S. et al. 2015. Abiotic and biotic controls of soil moisture spatiotemporal variability and the occurence of hysteresis. – Water Resour. Res. 51: 3505–3524.
Fatichi, S. et al. 2019. Modelling carbon sources and sinks in terrestrial vegetation. – New Phytol. 221: 652–668.
Fonti, P. et al. 2010. Studying global change through investigation of the plastic responses of xylem anatomy in tree rings. – New Phytol. 185: 42–53.
Friedlingstein, P. 2015. Carbon cycle feedbacks and future climate change. – Phil. Trans. R. Soc. A 373: 20140421.
Furze, M. E. et al. 2018. Detours on the phloem sugar highway: stem carbon storage and remobilization. – Curr. Opin. Plant Biol. 43: 89–95.
Good, S. P. et al. 2015. Hydrologic connectivity constrains partitioning of global terrestrial water fluxes. – Science 349: 175–177.
Granier, A. 1987. Evaluation of transpiration in a Douglas-fir stand by means of sap flow measurements. – Tree Physiol. 3: 309–320.
Hartl-Meier, C. et al. 2014. Mountain forest growth response to climate change in the northern Limestone Alps. – Trees 28: 819–829.
Hartmann, H. and Trumbore, S. 2016. Understanding the roles of nonstructural carbohydrates in forest trees – from what we can measure to what we want to know. – New Phytol. 211: 386–403.
Hartmann, H. et al. 2018. Research frontiers for improving our understanding of drought-induced tree and forest mortality. – New Phytol. 218: 15–28.
Hosking, J. R. M. 1984. Modeling persistence in hydrological time series using fractional differencing. – Water Resour. Res. 20: 1898–1908.
Huang, M. et al. 2018. Drought timing influences the legacy of tree growth recovery. – Global Change Biol. 24: 3546–3559.
Huntzinger, D. N. et al. 2017. Uncertainty in the response of terrestrial carbon sink to environmental drivers undermines carbon-climate feedback predictions. – Sci. Rep. 7: 1–8.
Hurst, H. 1951. Long-term storage capacity of reservoirs. – Trans. Am. Soc. Civ. Eng. 116: 770–799.
Jensen, K. H. et al. 2016. Sap flow and sugar transport in plants. – Rev. Mod. Phys. 88: 035007.
Katul, G. et al. 2001. Multiscale analysis of vegetation surface fluxes: from seconds to years. – Adv. Water Resour. 24: 1119–1132.
King, G. et al. 2013. Climatic drivers of hourly to yearly tree radius variations along a 6°C natural warming gradient. – Agric. For. Meteorol. 168: 36–46.
Kleinen, T. et al. 2003. The potential role of spectral properties in detecting thresholds in the Earth system: application to the thermohaline circulation. – Ocean Dyn. 53: 53–63.
Körner, C. 2013. Growth controls photosynthesis-mostly. – Nov. Acta Leopoldina 114: 3–13.

Koscielny-Bunde, E. et al. 1998. Indication of a universal persistence law governing atmospheric variability. – Phys. Rev. Lett. 81: 729–732.
Koutsoyiannis, D. 2015. Generic and parsimonious stochastic modelling for hydrology and beyond. – Hydrol. Sci. J. 6667: 1–6.
Le Quéré, C. et al. 2018. Global carbon budget 2017. – Earth Syst. Sci. Data 10: 405–448.
Lebourgeois, F. et al. 2010. Sensitivity of French temperate coniferous forests to climate variability and extreme events (*Abies alba*, *Picea abies* and *Pinus sylvestris*). – J. Veg. Sci. 21: 364–376.
Lévesque, M. et al. 2013. Drought response of five conifer species under contrasting water availability suggests high vulnerability of Norway spruce and European larch. – Global Change Biol. 19: 3184–3199.
Lloret, F. et al. 2011. Components of tree resilience: effects of successive low-growth episodes in old ponderosa pine forests. – Oikos 120: 1909–1920.
Lu, P. et al. 2004. Granier's thermal dissipation probe (TDP) method for measuring sap flow in trees: theory and practice. – Acta Bot. Sin. 46: 631–646.
Mahecha, M. D. et al. 2007. Characterizing ecosystem–atmosphere interactions from short to interannual time scales. – Biogeosciences 4: 743–758.
Mandelbrot, B. and Wallis, J. 1969. Some long-run properties of geophysical records. – Water Resour. Res. 5: 321–340.
Markonis, Y. and Koutsoyiannis, D. 2012. Climatic variability over time scales spanning nine orders of magnitude: connecting milankovitch cycles with Hurst–Kolmogorov dynamics. – Surv. Geophys. 34: 181–207.
Martinez-Vilalta, J. et al. 2016. Dynamics of non-structural carbohydrates in terrestrial plants: a global synthesis. – Ecol. Monogr. 86: 495–516.
Martinez-Vilalta, J. et al. 2018. Greater focus on water pools may improve our ability to understand and anticipate drought-induced mortality in plants. – New Phytol. 223: 22–32.
Mencuccini, M. et al. 2013. Concurrent measurements of change in the bark and xylem diameters of trees reveal a phloem-generated turgor signal. – New Phytol. 198: 1143–1154.
Mencuccini, M. et al. 2017. An empirical method that separates irreversible stem radial growth from bark water content changes in trees: theory and case studies. – Plant Cell Environ. 40: 290–303.
Mitchell, J. M. 1976. An overview of climate variability and its causal mechanisms. – Quat. Int. 6: 481–493.
Obojes, N. et al. 2018. Water stress limits transpiration and growth of European larch up to the lower subalpine belt in an inner-alpine dry valley. – New Phytol. 220: 460–475.
Ogle, K. et al. 2015. Quantifying ecological memory in plant and ecosystem processes. – Ecol. Lett. 18: 221–235.
Papoulis, A. 1965. Probability, random variables and stochastic processes. – McGraw-Hill.
Pappas, C. et al. 2017. Ecosystem functioning is enveloped by hydrometeorological variability. – Nat. Ecol. Evol. 1: 1263–1270.
Pappas, C. et al. 2018. Boreal tree hydrodynamics: asynchronous, diverging, yet complementary. – Tree Physiol. 38: 953–964.
Paschalis, A. et al. 2015. Cross-scale impact of climate temporal variability on ecosystem water and carbon fluxes. – J. Geophys. Res. Biogeosci. 120: 1716–1740.
Pelletier, J. D. and Turcotte, D. L. 1997. Long-range persistence in climatological and hydrological time series: analysis, modeling and application to drought hazard assessment. – J. Hydrol. 203: 198–208.
Peters, R. L. et al. 2015. Detecting long-term growth trends using tree rings: a critical evaluation of methods. – Global Change Biol. 21: 2040–2054.
Peters, R. L. et al. 2017. Contribution of climate vs. larch budmoth outbreaks in regulating biomass accumulation in high-elevation forests. – For. Ecol. Manage. 401: 147–158.
Peters, R. L. et al. 2018a. Quantification of uncertainties in conifer sap flow measured with the thermal dissipation method. – New Phytol. 219: 1283–1299.
Peters, R. L. et al. 2018b. Contrasting stomatal sensitivity to temperature and soil drought in mature alpine conifers. – Plant. Cell Environ. 42: 1674–1689.
Pfautsch, S. 2016. Hydraulic anatomy and function of trees – basics and critical developments. – Curr. For. Rep. 2: 236–248.
Reichstein, M. et al. 2013. Climate extremes and the carbon cycle. – Nature 500: 287–295.
Reyer, C. P. O. et al. 2013. A plant's perspective of extremes: terrestrial plant responses to changing climatic variability. – Global Change Biol. 19: 75–89.
Richardson, A. D. et al. 2010. Influence of spring and autumn phenological transitions on forest ecosystem productivity. – Phil. Trans. R. Soc. B 365: 3227–3246.
Richardson, A. D. et al. 2013. Seasonal dynamics and age of stemwood nonstructural carbohydrates in temperate forest trees. – New Phytol. 197: 850–861.
Rogers, B. M. et al. 2018. Detecting early-warning signals of tree mortality in boreal North America using multiscale satellite data. – Global Change Biol. 24: 2284–2304.
Sass-Klaassen, U. et al. 2016. A tree-centered approach to assess impacts of extreme climatic events on forests. – Front. Plant Sci. 7: 1–6.
Scheffer, M. et al. 2015. Generic indicators of ecological resilience: inferring the chance of a critical transition. – Annu. Rev. Ecol. Evol. Syst. 46: 145–167.
Schlesinger, W. H. and Jasechko, S. 2014. Transpiration in the global water cycle. – Agric. For. Meteorol. 189–190: 115–117.
Schulze, E. et al. 1985. Canopy transpiration and water fluxes in the xylem of the trunk of *Larix* and *Picea* trees – a comparison of xylem flow, porometer and cuvette measurements. – Oecologia 66: 475–483.
Serra-Maluquer, X. et al. 2018. Changes in tree resistance, recovery and resilience across three successive extreme droughts in the northeast Iberian Peninsula. – Oecologia 187: 343–354.
Simard, S. et al. 2013. Intra-annual dynamics of non-structural carbohydrates in the cambium of mature conifer trees reflects radial growth demands. – Tree Physiol. 33: 913–923.
Steppe, K. et al. 2010. A comparison of sap flux density using thermal dissipation, heat pulse velocity and heat field deformation methods. – Agric. For. Meteorol. 150: 1046–1056.
Steppe, K. et al. 2015. Diel growth dynamics in tree stems: linking anatomy and ecophysiology. – Trends Plant Sci. 20: 335–343.
Stoy, P. C. et al. 2005. Variability in net ecosystem exchange from hourly to inter-annual time scales at adjacent pine and hardwood forests: a wavelet analysis. – Tree Physiol. 25: 887–902.
Taqqu, M. et al. 1995. Estimators for long-range dependence: an empirical study. – Fractals 3: 785–798.

Theurillat, J. and Guisan, A. 2001. Potential impact of climate change on vegetation in the European Alps: a review. – Clim. Change 50: 77–109.
Trumbore, S. et al. 2015. Forest health and global change. – Science 349: 814–818.
van de Leemput, I. A. et al. 2018. Slow recovery from local disturbances as an indicator for loss of ecosystem resilience. – Ecosystems 21: 141–152.
Venturas, M. D. et al. 2017. Plant xylem hydraulics: what we understand, current research and future challenges. – J. Integr. Plant Biol. 59: 356–389.

Supplementary material (available online as Appendix ecog-04968 at <www.ecography.org/appendix/ecog-04968>). Appendix 1–3.

von Arx, G. and Carrer, M. 2014. Roxas – a new tool to build centuries-long tracheid-lumen chronologies in conifers. – Dendrochronologia 32: 290–293.
Wu, C. et al. 2013. Interannual variability of net ecosystem productivity in forests is explained by carbon flux phenology in autumn. – Global Ecol. Biogeogr. 22: 994–1006.
Zweifel, R. et al. 2001. Link between diurnal stem radius changes and tree water relations. – Tree Physiol. 21: 869–877.
Zweifel, R. et al. 2016. Are trees able to grow in periods of stem shrinkage? – New Phytol. 211: 839–849.